Derivative Based Focal Plane Array Nonuniformity Correction

G. Ness, A. Oved, I. Kakon
Electro Optics Department, RAFAEL PO Box 2250 (39) Haifa 31021, ISRAEL

This paper presents a fast and robust method for fixed pattern noise nonuniformity correction of infrared focal plane arrays. The proposed method requires neither shutter nor elaborate calibrations and therefore enables a real time correction with no interruptions. Based on derivative estimation of the fixed pattern noise from pixel sized translations of the focal plane array, the proposed method has the advantages of being invariant to the noise magnitude and robust to unknown camera and inter-scene movements while being virtually transparent to the end-user.

arXiv:1702.06118v1 [cs.CV] 19 Feb 2017

Infrared focal-plane arrays (FPA) are used in a plethora of imaging systems designed for various applications. Although FPA fabrication techniques are constantly improving, their performance is still greatly affected by fixed pattern noise (FPN). This is in principle an undesired spatially varying bias and gain terms (higher order terms are usually negligible). While each detector's response (gain term) is usually temporally constant, its bias term tends to drift significantly over time due to temperature variations of the FPA and its surroundings. FPN in infrared imaging systems severely deteriorates image quality which affects both human observer and machine vision based tasks, and therefore must be addressed accordingly. Over the years, many algorithms and calibration schemes were introduced in order to estimate and correct FPN. They can be categorized into two groups: calibration based and scene based algorithms.

Calibration based algorithms usually provide satisfactory results, they require either long and costly calibration or repetitive interruption to the imaging process. The most widely used calibration based technique [1] which known as one point correction, is achieved by placing a uniformly distributed radiation source (opaque shutter, de-focusing etc.) in front of the FPA, and by doing so obscuring the scene from the FPA. Since the radiation is uniformly distributed across the FPA, any residual pattern at this stage is attributed to the unknown bias and is easily compensated by subtracting it from all following frames.

More accurate correction can be achieved by compensating for the gain nonuniformity in addition to the bias nonuniformity. In contrast to the temporally varying bias term, the gain term is usually constant and can be calibrated once. More sophisticated calibration schemes [2, 4–10] are also available which enable to maintain low FPN levels for relatively long operation times. The main drawback of those schemes is the long and costly calibration process involved.

A second group of FPN estimation techniques is the scene based nonuniformity correction (NUC) [11–13]. In principle, scene based NUC methods rely on a sequence of frames taken at different imaging conditions (scene change, varying integration time, varying the imaging direction etc.). Since the FPN and the imaged scene are uncorrelated, it is possible to algorithmically separate the scene from the FPN. Naturally, the scene based approach is favorable since it neither requires long calibrations nor interfere with the continuous imaging of the scene. [14, 15] show that the mean and the standard deviation of the signal calculated over a large collection of frames at each detector are its offset and gain respectively. In [16], the advantage of constant statistics is taken for estimating the FPN. In [17], a neural network approach and retina like processing techniques suggested to estimate the FPN. Different approach [18, 19] uses frames produced by dithering the detector in a known pattern. Our approach can be classified as a scene based paper approach, yet it differs from a systemic standpoint, as it enables accurate and robust reconstruction of the FPN from its derivatives. The FPN derivatives are estimated using frames captured during FPA translations, or during angular movements of the entire imaging system.

In this paper, we describe the model of FPN reconstruction review numerical simulation and present experimental results of the algorithm.

Let $\widetilde{R}_n(i,j)$ be the raw value of the pixel $[i,j]$ located at the i^{th} row and j^{th} column of the n^{th} frame. A simple imaging model for pixel $[i,j]$ can be

$$\widetilde{R}_n(i,j) = \phi_n(i,j) \cdot g_n(i,j) + \widetilde{o}_n(i,j) + \eta \,, \quad (1)$$

where $\phi_n(i,j)$ is the radiance emitted from the scene, integrated over the pixel's active area within the frame integration time. $g(i,j)$ and $\widetilde{o}_n(i,j)$ describe the pixel gain and offset respectively. η is the temporal noise term, which will be neglected in further calculations for simplicity of description and will be reduced by temporal averaging (the distortion caused by temporal noise was evaluated by simulation). We assume that the FPN estimation process is short enough so that the offset term is considered temporally constant during the correction process, that is $\widetilde{o}_n(i,j) \equiv \widetilde{o}(i,j)$. We also assume that the gain term is known from previous calibration stage, therefore we can simplify Eq. 1 by compensating for the gain nonuniformity. This is achieved by multiplying both sides of Eq. 1 by $g(i,j)^{-1}$:

$$R_n(i,j) = \phi_n(i,j) + o(i,j) \,, \quad (2)$$

where

$$\begin{cases} R_n(i,j) \equiv \widetilde{R}_n(i,j) \cdot g(i,j)^{-1} \\ o(i,j) \equiv \widetilde{o}(i,j) \cdot g(i,j)^{-1} \end{cases} .$$

Figure 1: The scene as it captured before and after the transverse shift

After frame n is captured, we physically shift the FPA by a single pixel-sized step. Without lost of generality we shall first describe dithering in the horizontal direction, leading to the next frame

$$R_{n+1}(i,j) = \phi_{n+1}(i,j+1) + o(i,j) \ . \tag{3}$$

The shifting process is described graphically in Fig. 1. Based on frames n and $n+1$, we can now calculate two differences:

- Temporal difference (Δ_t) between raw frame $n+1$ (Eq. 3) and raw frame n (Eq. 2)

$$\begin{aligned}\Delta_t(R_n(i,j)) &\equiv R_{n+1}(i,j) - R_n(i,j) \\ &= \phi_{n+1}(i,j+1) - \phi_n(i,j) \ .\end{aligned} \tag{4}$$

- Discrete horizontal derivative (Δ_x) of raw frame n (Eq. 2)

$$\begin{aligned}\Delta_x(R_n(i,j)) &\equiv R_n(i,j+1) - R_n(i,j) \\ &= \phi_n(i,j+1) - \phi_n(i,j) + o(i,j+1) - o(i,j) \ .\end{aligned} \tag{5}$$

Subtraction of Eq. 4 from Eq. 5 results:

$$\begin{aligned}&\Delta_x(R_n(i,j)) - \Delta_t(R_n(i,j)) \\ &\quad = [o(i,j+1) - o(i,j)] \\ &\quad - [\phi_{n+1}(i,j+1) - \phi_n(i,j+1)] \ ,\end{aligned} \tag{6}$$

which can be rewritten as:

$$\begin{aligned}&\Delta_x(R_n(i,j)) - \Delta_t(R_n(i,j)) \\ &\quad = \Delta_x(o(i,j)) - \Delta_t(\phi_n(i,j+1)) \ ,\end{aligned} \tag{7}$$

where $\Delta_x(o(i,j))$ is the FPN discrete horizontal derivative and $\Delta_t(\phi_n(i,j+1))$ is the scene temporal difference. After frame $n+1$ is captured, the FPA is shifted back to its original position.

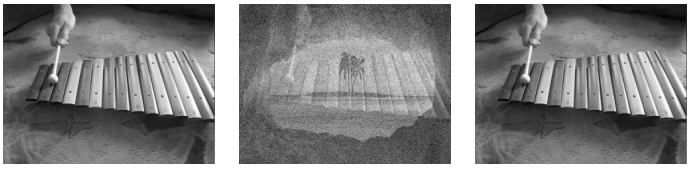

(a) Original frame (b) Corrupted frame (c) Corrected frame

Figure 2: Algorithm simulation

Since $\Delta_t(\phi_n(i,j+1))$ is usually small for typical frame rate and since $\Delta_x(o(i,j))$ and $\Delta_t(\phi_n(i,j+1))$ are uncorrelated, we can filter out $\Delta_t(\phi_n(i,j+1))$ by computing Eq. 7 temporal median for several cycles, leading to estimation of the FPN horizontal derivative $\Delta_x(o(i,j))$.

Similarly, the entire process is repeated for the vertical direction, leading to an estimation of the FPN vertical derivative $\Delta_y(o(i,j))$.

The last stage is the reconstruction of the FPN from the estimated spatial derivatives. In one dimension, the reconstruction of a signal from its derivatives is achieved by simple integration. The two dimensional case is different since the estimated gradient vector field isn't necessarily integrable. In other words, there might not exist a surface such that $[\Delta_x(o), \Delta_y(o)]$ is its gradient field. In such a case, we seek for a surface $\tilde{o}(i,j)$ so that $\sum_{i,j} |\nabla\tilde{o}(i,j) - (\Delta_x(o(i,j)), \Delta_y(o(i,j)))|$ is minimal. There are several algorithms addressing this problem, including the projection of the estimated gradient field onto a finite set of orthonormal basis functions and other iterative solvers [20, 21].

Applying additional derivative on the gradient map and summing both vector components, is equivalent to applying the Laplace operator on the (*a priory* unknown) offset map. In order to reconstruct the FPN, we need to solve the Poisson equation:

$$(\Delta_x, \Delta_y) \cdot (\Delta_x(o(i,j)), \Delta_y(o(i,j)))^\top = \nabla^2 o(i,j) \tag{8}$$

This can be transformed into the frequency domain, by projecting the estimated derivatives on an integrable set of functions, and solved by integrating the projected set instead [22]. Selection of the specific set of integrable functions should be done according to the problem constraints. We chose to project on the complete set of cosines, that is the solution of the Poisson equation under Neumann boundary conditions.

We have tested and measured the robustness of the method using simulated dithering of virtual FPA. We used standard 240×320 pixels video of normalized standard deviation. FPN was introduced by means of sample picture which includes high and low spatial frequencies as well as an extra constant random noise per pixel. The original video frames were shifted over FPN as temporal random noise was added. In Fig. 2, we present original (Fig. 2a), corrupted (Fig. 2b) and corrected (Fig. 2c) arbitrary video frame.

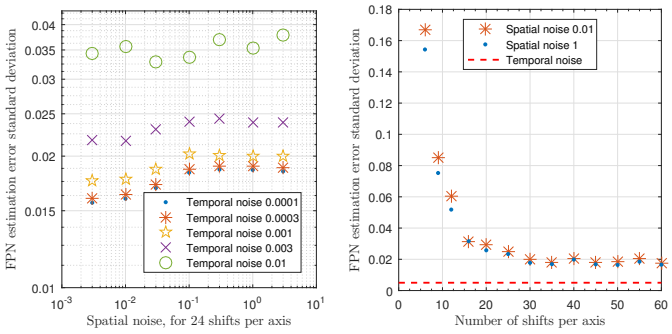

(a) (b)

Figure 3: **a**. Residual correction error vs. FPN strength, for several temporal noises. One can notice the error kept small even for strong FPN. **b**. Error vs. number of shifts, for several spatial noises. One can notice the error decrease with the shifts number and the weak dependence of spatial noise strength.

The residual error enumerated by standard deviation for the difference between estimated and actual FPN, normalized by the standard deviation of the scene. Error was calculated for various conditions of spatial noise (FPN strength over original frame), temporal noise and number of dithering repetitions, as in Fig. 3a and 3b. Notice that the error is only slightly dependent of the spatial noise for various temporal noise (as expected since there was no assumption for weak spatial noise), as can be noticed in Fig. 3a and 3b. The reconstruction performance increases as more frames are used (Fig. 3b).

Next we shall explore shift magnitude errors (as may caused by mechanical apparatuses), in sub-pixel level. We used typical values of spatial noise, temporal noise and number of shifts per axis (0.1, 0.0003 and 32 respectively), and compared the estimated FPN for different mean and standard deviations of the translations. It should be mentioned that the shift errors simulated as normally distributed random translations (around the mean in the longitudinal direction and around zero in the transverse direction). As shown in Fig. 4, the estimation seems to keep its accuracy even for significant shift errors.

We have demonstrated the method using microbolometer of 640×480 pixels, over complex and dynamic scene, which included both near and far objects, having relative motion. High and low spatial frequencies appeared in the scene. For convenience, the process previously introduced was slightly modified, as the repetitive single pixel shift altered by a constant angular velocity pitch and yaw of the entire imaging system. This movement is equivalent to a transverse translations of the FPA under the assumption of zero distortion system: If we set the angular velocity to be the instantaneous field of view multiplied by the frame rate, we get an effective single pixel shift per frame of the imaged scene with respect to the sensor.

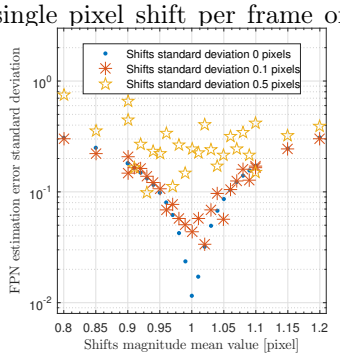
FPN estimation error standard deviation
Shifts magnitude mean value [pixel]
Shifts standard deviation 0 pixels
Shifts standard deviation 0.1 pixels
Shifts standard deviation 0.5 pixels

Figure 4: Residual error of the corrected FPN vs. applied shifts mean, for several shifts standard deviations.

In Fig. 5, we present the raw signal from the camera (Fig. 5a), the proposed method correction (Fig. 5b) and the conventional bias and gain correction (Fig. 5c).

We present a method for FPN correction based on minute transverse shifts of the FPA, which is robust to unexpected camera shakes and interscene movements, provided with a demonstration of the algorithm performance and accuracy in a complex scene. Implementation of this algorithm can be applied using a transverse shift of the FPA or angular movement of the optical axis. Although the proposed method has been tested on uncooled microbolometer, it can be applied on any detector suffering from either FPN or slowly varying noise of any magnitude within the dynamic range, as long as single pixel shift is possible. Therefore, it eliminates the need of long and costly calibrations and mechanical mechanisms.

ACKNOWLEDGMENT

The authors thank Ami Yaacobi, Eli Minkov and Ephi Pinnsky for their support and assistance with this model. Special thanks also go to Yohai Barnea, Pavel Bavly, Daniel Dahan and Yotam Ater for their technical support.

[1] G. C. Holst, "CCD Arrays, Cameras and Displays, " SPIE Optical Eng. Press, 1996.

[2] M. Schulz, and L. Caldwell, "Nonuniformity correction and correctability of infrared focal plane arrays." SPIE's 1995 Symposium on OE/Aerospace Sensing and Dual Use Photonics. International Society for Optics and Photonics, 1995.

[3]

(a) Raw signal (b) Correction using proposed method (c) Conventional correction

Figure 5: Results comparison

[4] A.F. Milton, F. R. Barone, M. R. Kruer, "In of Nonuniformity on Infrared Focal Plane Array Performance, " SPIE Opt. Eng., vol. 24, pp. 855-862, 1985.

[5] D. A. Scribner, J. T. Caulfield, K. A. Sarkady, M. R. Kruer, and J. D. Hunt, "An Imaging Metric for Infrared Focal-Plane Arrays, " Proc. SPIE, vol. 1686, 1992.

[6] D. L. Perry and E. L. Dereniak, "Linear Theory of Nonuniformity Correction in Infrared Staring Sensors, " SPIE Opt. Eng., vol. 32, pp. 1853-1859, 1993.

[7] Y. Xianghui, W. Wenlue, and Z. Mingfu, "New Method for Nonuniformity Correction of Solid State Image Sensor, " Proc. SPIE, vol. 2564, 1995.

[8] M. Schulz and L. Calwell, "Nonuniformity Correction and Correctability of Infrared Focal Plane Arrays, " Infrared Phys. Technol., vol. 36, pp. 763-777, 1995.

[9] W. Gross, T. Hierl, and M. Schulz, "Correctability and Long-Term Stability of Infrared Focal Plane Arrays, SPIE Opt. Eng., vol. 38, pp. 862-869, 1999.

[10] J. McBride and M. Snorrason. "Improving scene-based nonuniformity correction for infrared images using frequency domain processing." SPIE Defense, Security, and Sensing. International Society for Optics and Photonics, 2009.

[11] E. Vera, P. Meza, and S. Torres, "Total variation approach for adaptive nonuniformity correction in focal-plane arrays," Opt. Lett. 36, 172-174 (2011)

[12] C. Liang, H. Sang, and X. Shen, "Efficient scene-based method for real-time non-uniformity correction of infrared video sequences." Electronics papers 50.12 (2014): 868-870.

[13] A. Kumar, "Sensor non uniformity correction Algorithms and its real time Implementation for Infrared Focal Plane Array-based thermal Imaging System." Defence Science Journal 63.6 (2013): 589-598.

[14] Y. Bae et al., "Scene-based nonuniformity correction in infrared videos." SPIE Defense, Security, and Sensing. International Society for Optics and Photonics, 2012.

[15] P. M. Narendra and N. A. Foss, "Shutterless Fixed Pattern Noise Correction for Infrared Imaging Arrays, " Proc. SPIE, vol. 282, pp. 44-51, 1981.

[16] L. Geng et al., "An improvement for scene-based nonuniformity correction of infrared image sequences." ISPDI 2013-Fifth International Symposium on Photoelectronic Detection and Imaging. International Society for Optics and Photonics, 2013.

[17] Rui, Lai, et al. "Improved neural network based scene-adaptive nonuniformity correction method for infrared focal plane arrays." Applied optics 47.24 (2008): 4331-4335.

[18] W. F. O'Neil, "Dithered Scan Detector Compesation, " Proc. IRIS, 1993.

[19] W. F. O'Neil, "Experimental Verification of Dithered Scan Non-Uniformity Correction, " Proc. IRIS, 1997.

[20] R. T. Frankot and R. Chellappa. "A method for enforcing integrability in shape from shading algorithms." Pattern Analysis and Machine Intelligence, IEEE Transactions on 10.4 (1988): 439-451.

[20] M. Kazhdan, M. Bolitho and H. Hoppe. "Poisson surface reconstruction." Proceedings of the fourth Eurographics symposium on Geometry processing. Vol. 7. 2006.

[21] M. Rostami, O. V. Michailovich and Z. Wang. "Surface reconstruction in gradient-field domain using compressed sensing." Image Processing, IEEE Transactions on 24.5 (2015): 1628-1638.

[22] A. Agrawal, R. Raskar and R. Chellappa. "What is the range of surface reconstructions from a gradient field?." Computer Vision–ECCV 2006. Springer Berlin Heidelberg, 2006. 578-591.